Thermodynamic Analysis of Degenerate Recognition by the NKG2D Immunoreceptor: Not Induced Fit but Rigid Adaptation

Benjamin J. McFarland¹ and Roland K. Strong* The Division of Basic Sciences Fred Hutchinson Cancer Research Center 1100 Fairview Avenue N. Seattle, Washington 98109

Summary

The homodimeric immunoreceptor NKG2D drives the activation of effector cells following engagement of diverse, conditionally expressed MHC class I-like protein ligands. NKG2D recognition is highly degenerate in that a single surface on receptor monomers binds pairs of distinct surfaces on each structurally divergent ligand, simultaneously accommodating multiple nonconservative ligand allelic or isoform substitutions. In contrast to TCR-pMHC and other NK receptor-ligand interactions, thermodynamic and kinetic analyses of four NKG2D-ligand pairs (MIC-A*001, MIC-B*005, ULBP1, and RAE-1β) reported here show that the relative enthalpic and entropic terms, heat capacity, association rates, and activation energy barriers are comparable to typical, rigid protein-protein interactions. Rather than "induced-fit" binding, NKG2D degeneracy is achieved using distinct interaction mechanisms at each rigid interface.

Introduction

The C-type lectin-like immunoreceptor NKG2D is an outlier member of the NKG2x-CD94 family (x = A, B, C,E, and H) in terms of sequence, distribution, multimeric state, and function. NKG2D was first functionally defined as an activating receptor on natural killer (NK) cells mediating responses to the stress-induced expression of the MIC family of MHC class I-like ligands on intestinal epithelial cells (Bauer et al., 1999). Subsequently, NKG2D has been shown to be broadly expressed, playing additional roles in innate immunity by driving the activation of macrophages (Diefenbach et al., 2000) and particular $\gamma\delta$ T cell populations (Das et al., 2001), and in adaptive immunity by providing costimulatory signals to CD8 $^+$ $\alpha\beta$ T cells (Groh et al., 2001). NKG2D engagement initiates perforin-mediated cytolytic responses against virally infected and tumorigenic cells (Cerwenka and Lanier, 2001; Hayakawa et al., 2002). NKG2D is therefore a potent mediator of antiviral and antitumor immunosurveillance. Tumor cells can evade this immunosurveillance by producing soluble MIC ligands, shed through proteolysis, resulting in downregulation of NKG2D cell surface expression on immune effector cells (Groh et al., 2002; Salih et al., 2002). To accomplish these functions, NKG2D interacts with a diverse array of distinct MHC class I-homologous ligands: in humans, the closely related, polymorphic proteins MIC-A and MIC-B (Steinle et al., 2001), ULBP1, 2, 3, and 4 (Cosman et al., 2001; Jan Chalupny et al., 2003), and MULT1 (Carayannopoulos et al., 2002a); in mice, RAE-1 α , β , γ , and δ (Carayannopoulos et al., 2002b), H60 (O'Callaghan et al., 2001) and possibly *Mill1* and *2* (proposed on the basis of homology to MIC; Kasahara et al., 2002). While murine (muNKG2D) and human NKG2D (huNKG2D) are highly conserved (69% identical in the ectodomains), and the NKG2D ligands are well conserved within families (ranging from 55% identity among the ULBPs to greater than 84% between MIC-A and -B alleles), the ligands are distantly related between families in terms of both sequence (23% to 27% identical) and detailed structure.

Crystal structures are available for muNKG2D and huNKG2D, free (McFarland et al., 2003; Wolan et al., 2001) or bound to either MIC-A (allele 001; Li et al., 2001), ULBP3 (Radaev et al., 2001), or RAE-1β (Li et al., 2002). These structures show the homodimeric receptor interacting with monomeric ligands in similar 2:1 complexes, with an equivalent surface on each NKG2D monomer binding intimately to pairs of distinct surfaces on the asymmetric ligands, on either the $\alpha 1$ or $\alpha 2$ domains, yielding six distinct receptor-ligand interfaces. The footprint and overall arrangement of the NKG2D-ligand complexes is strongly reminiscent of $\alpha\beta$ TCR-peptide-MHC class I (TCR-pMHC) complexes, though the NKG2Dmediated recognition events are tighter, more extensive. more shape-complementary, and involve the C-type lectin-like domains of NKG2D rather than the immunoglobulin-like domains of TCRs. Where MHC class I polymorphic and antigenic peptide sequence differences in the binding footprint result directly in differential recognition by the constellation of TCRs in a host, NKG2D recognition conversely tolerates dramatic allelic (MIC) and isoform (ULBP and RAE-1) differences in contact residues with only minor changes in affinity (McFarland et al., 2003; O'Callaghan et al., 2001; Steinle et al., 2001; Strong, 2002).

This extreme recognition degeneracy (α 1 versus α 2 on a ligand protein, one ligand protein versus another, surfaces remodeled through substitution) is not accomplished through dominance of electrostatic or hydrophobic interactions, which are relatively insensitive to precise geometry and therefore enable degenerate binding, exemplified by chemokine-receptor interactions (Alexander et al., 2002; Skelton et al., 1999) and in the binding of human growth hormone to hormone and prolactin receptors (Clackson and Wells, 1995; Somers et al., 1994). Solvent is also cleanly excluded from the interfaces, disallowing variable water-mediated contacts as a means for achieving degeneracy. Conformational plasticity, or "induced-fit" recognition, where a flexible binding site can mold to accommodate diverse ligands, is typical of many antibody-antigen interactions (James et al., 2003; Sundberg and Mariuzza, 2000) and has been invoked to account for TCR-pMHC crossreactivity (Wu et al., 2002). Structural comparisons of NKG2D-ligand complexes have been alternately interpreted as sug-

^{*}Correspondence: rstrong@fhcrc.org

¹Present address: Department of Chemistry and Biochemistry, Seattle Pacific University, 3307 Third Avenue West, Seattle, Washington 98119.

gesting that flexibility, and thus induced-fit binding, does (Radaev et al., 2001, 2002) or does not (McFarland et al., 2003) significantly contribute to NKG2D recognition degeneracy.

Here we show that the binding energetics of four NKG2D-ligand complexes are incompatible with standard definitions of induced-fit binding but are completely consistent with conventional rigid protein-protein interactions in general and the lack of observed flexibility at the NKG2D binding sites specifically (McFarland et al., 2003). We conclude that NKG2D degeneracy is rather achieved by an extreme example of the degenerate binding mechanism first fully documented for the interactions between diverse proteins and a common site on immunoglobulin Fc regions-a mechanism we term "rigid adaptation," in which a rigid binding site on NKG2D makes diverse interactions with a series of chemically and structurally distinct ligand surfaces by utilizing a core set of residues capable of multifarious bonds.

Results

Thermodynamic Analysis

Induced-fit binding is a prominent feature of many immunological receptor-ligand interactions, including some antibodies (Rini et al., 1992; Sundberg and Mariuzza, 2002) and $\alpha\beta$ TCRs (Garcia et al., 1998; Reiser et al., 2002). Detailed thermodynamic and kinetic studies, either by surface plasmon resonance (SPR) or isothermal titration calorimetry (ITC), have provided direct biophysical evidence for induced-fit binding mechanisms (reviewed in Rudolph et al., 2002, and Sundberg and Mariuzza, 2002). For induced-fit TCR-pMHC interactions, slow on-rates are typically compensated for by slow off-rates, delivering reasonable absolute affinities. This characteristic behavior of induced-fit mechanisms results from high entropic barriers to forming an ordered transition state (Willcox et al., 1999); unfavorable entropy changes (ΔS°) upon binding, compensated for by favorable enthalpic terms (ΔH°) (Boniface et al., 1999); and large changes in heat capacities, close to 1 kcal/mol K, due to the ordering of flexible ligand binding sites upon binding, with concomitant burial of protein surface and release of previously ordered water molecules (Spolar and Record, 1994).

In order to determine the role that flexibility and induced-fit binding plays in NKG2D recognition, the energetic parameters for four NKG2D-ligand pairs (MIC-A, MIC-B, ULBP1, and RAE-1 β) were determined using an SPR-based methodology inspired by comparable analyses of three $\alpha\beta$ TCR-pMHC interactions (Boniface et al., 1999; Willcox et al., 1999). In these analyses, binding energy is broken down into separate enthalpic (Δ H°) and entropic (Δ S°) contributions by either conventional (plotting lnK $_{\rm D}$ versus the reciprocal of temperature [1/T] [Willcox et al., 1999]) or three-parameter (curve-fitting plots of Δ G° versus T [Boniface et al., 1999]) van't Hoff methodology. Energetic terms are derived from an expansion of the Gibbs free energy (Δ G°), the change in free energy upon binding:

$$\Delta \mathbf{G}^{\circ} = \Delta \mathbf{H}^{\circ} - \mathbf{T} \Delta \mathbf{S}^{\circ} \tag{1}$$

Curvature in a plot of ΔG° versus T shows that ΔH° and ΔS° change with temperature according to a third parameter, the heat capacity (ΔC°_{P}):

$$\Delta \textbf{H}^{\circ}_{\ \textbf{T}} = \Delta \textbf{H}^{\circ}_{\ \textbf{T}_{R}} + \Delta \textbf{C}^{\circ}_{\ \textbf{P}} \ (\textbf{T} \ -\textbf{T}_{\textbf{R}}) \label{eq:deltaH} \tag{2}$$

and

$$\Delta S^{\circ}_{T} = \Delta S^{\circ}_{T_{R}} + \Delta C^{\circ}_{P} \ln(T/T_{R})$$
 (3)

where T_R is a reference temperature, commonly 298 K (see Experimental Procedures). According to an analysis of protein folding, protein-protein, and protein-DNA interactions (Spolar and Record, 1994), ΔC_P° is directly related to the change in flexible, exposed protein surface upon binding and allows an estimate of the change in conformational entropy upon binding (ΔS°_{other} , which is estimated at T_s , the temperature where $\Delta S^{\circ} = 0$; see Experimental Procedures). The absolute accuracy of this method depends on the model relating buried polar/ nonpolar surface area to heat capacity (Henriques et al., 2000), but the comparative analysis of NKG2D-ligand with TCR-pMHC thermodynamics reported here should be insensitive to such effects: the interfaces are chemically similar (polar/nonpolar ratio) and an identical methodology, SPR, has been used under identical buffer and temperature conditions.

NKG2D-Ligand Interactions Are Driven by Both Enthalpy and Entropy

Conventional van't Hoff analysis has been used to determine the enthalpies for two TCR-pMHC interactions, JM22z-HLA-A2-flu (human) and F5z-H2-Db-NP (mouse) (Willcox et al., 1999), where entropies (in the form of $T\Delta S^{\circ}$) were subsequently determined by subtraction of ΔH° from ΔG° . Since these terms are treated as constants in conventional van't Hoff analyses, the change in heat capacity of the system was assumed to be zero. For the JM22z-HLA-A2-flu interaction, values of ΔH° and ΔS° obtained by a conventional van't Hoff analysis of SPR data compared favorably (within \sim 20%) to those directly measured by ITC (Willcox et al., 1999) (Table 1), validating the use of SPR to estimate binding thermodynamics. ΔH° , ΔS° , and ΔC°_{P} for the 2B4-H2-IE^{k-}MCC (mouse) TCR-pMHC interaction were determined by a three-parameter van't Hoff analysis of SPR data (Boniface et al., 1999). We used both analysis methods to derive the thermodynamic parameters for four NKG2Dligand complexes (Figures 1C and 1D and Table 1). The results of both methods agree to within two kcal/mol. confirming that heat capacity changes for NKG2D-ligand complexation are relatively minor, but the expanded parameterization clearly provides better fits of the data for several of the complexes.

Both van't Hoff fitting methods segregate NKG2D-ligand interaction energy into substantially favorable entropic and enthalpic components (Table 1). For all four ligands, entropy drives the complexation of NKG2D more than enthalpy so that the disorder in the system has actually increased upon binding, presumably in part due to release of ordered water from buried surfaces. While conventional van't Hoff estimations of thermodynamic parameters are valid only near the middle of the temperature range (here, as in most thermodynamic

Table 1	Cummon	of Thorma	advinamia.	Parameters 1 4 1	0+ 0E°C

NKG2D-Ligand	K_D (μM) a	$\Delta G^{\circ} \ (^{kcal} /_{mol})^{b}$	ΔH° (*cal/mol)c	$T\DeltaS^\circ$ (kcal/mol)c	$\Delta {\sf H}^{\circ}{}_{\sf VH} \; (^{\sf kcal}/_{\sf mol})^{\sf d}$	$T\Delta S^{\circ}_{VH}(^{kcal/_{mol}})^{d}$
MIC-A	0.94 ± 0.13	-8.2	-1.6 ± 0.6	6.7 ± 0.6	-0.1 ± 0.8	8.1
MIC-B	0.79 ± 0.03	-8.3	-1.1 ± 0.6	7.3 ± 0.6	-0.6 ± 0.6	7.8
ULBP1	1.1 ± 0.2	-8.1	-2.9 ± 0.6	5.3 ± 0.6	-2.4 ± 0.6	5.7
RAE-1β	1.9 ± 0.2	-7.8	-3.3 ± 0.3	4.5 ± 0.3	-2.8 ± 0.3	5.0
RAE-1δ°	0.49 ± 0.10	-8.6	_	_	-5.2	3.4
TCR-MHC-Peptide						
JM22z-HLA-A2-fluf	6.6 ± 2	−7.1	-19.7 ± 1.4	-12.6	-23	-15.9
F5z-H2-Db-NPf	11	-6.7	_	_	-19	-12.3
2B4-H2-E ^k -MCC ^g	6.6	−7.1	-12.7 ± 0.2	-5.6 ± 0.2	_	_
172.10-H2-A ^u -MBP1 ^h	17	-6.9	-21.2	-14.3	_	_
1934.4-H2-A ^u -MBP1 ^h	320	-6.0	-15.7	-9.6	_	_
D3-HLA-A2-SL9i	24	−7.5	-10.4	-2.9	_	_

^a Errors calculated from standard deviation of three to four independent equilibrium binding experiments.

analyses using SPR, around 25°C), explicit calculation of the heat capacity allows estimation of thermodynamic parameters throughout the range. At 37°C, according

to equations 2 and 3, the MIC-B, ULBP1, and RAE- 1β interactions with NKG2D are still driven by both enthalpy and entropy, although now enthalpy has become domi-

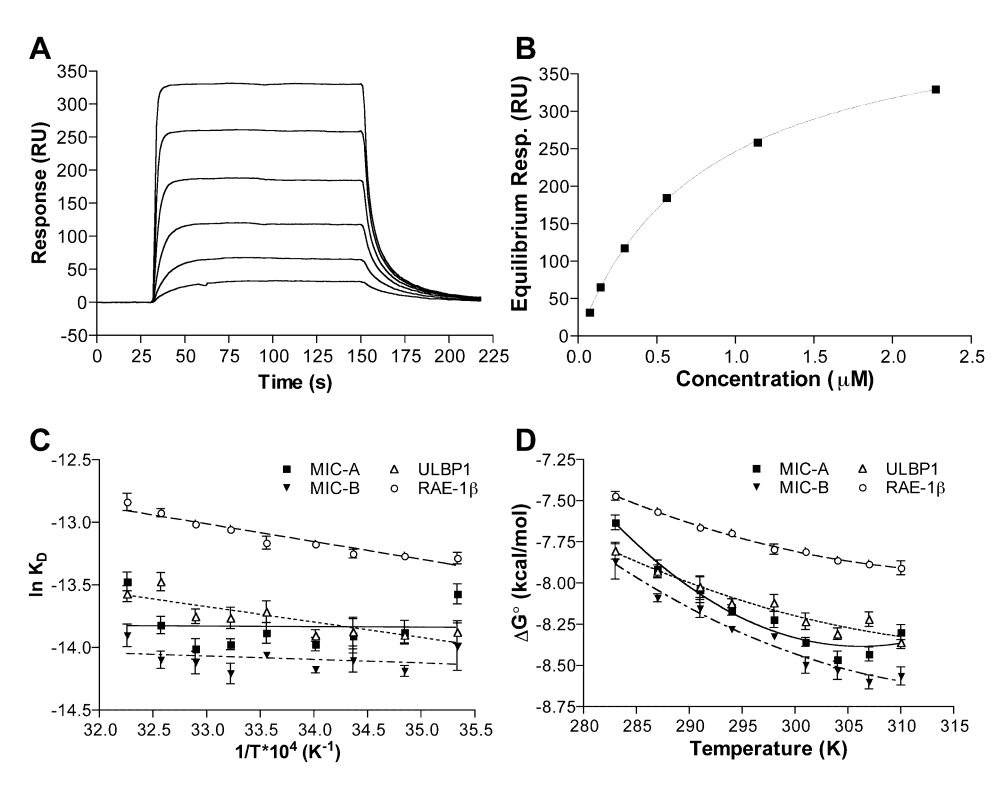


Figure 1. Determination of Thermodynamic Parameters through Two Fitting Methods

- (A) NKG2D was injected at 15 μ l/min over a MIC-B-coupled dextran surface in six serial dilutions ranging from 2.3 μ M to 0.06 μ M at 298 K. The response of an in-line HLA-G control surface was subtracted. Response at equilibrium was measured as an average of 10 to 20 s of data collected near the end of the injection.
- (B) Plot of response of MIC-B surface versus [NKG2D]. The equation fit to the data was Response = $K_A \times [NKG2D] \times R_{max}/(K_A \times [NKG2D] + 1)$; $K_D = 1/K_A$. R_{max} is the saturation response of the chip.
- (C) Van't Hoff plots for huNKG2D interacting with MIC-A, MIC-B, ULBP1, and muNKG2D interacting with RAE-1β.
- (D) Three-parameter fits to the same data with K_{D} converted to $\Delta G^{\circ}.$

 $^{{}^{}b}\Delta G^{\circ} = -RT \ln (K_{D})$

 $^{^{}c}\Delta H^{o}$ and ΔS^{o} determined from three-parameter fit, with standard error of fit reported; $T_{B}=298$ K.

 $^{^{}d}\Delta \text{H}^{\circ} \text{ determined from slope of van't Hoff plot, with standard error from fit reported; } T\Delta S^{\circ}_{\text{VH}} = \Delta \text{H}^{\circ}_{\text{VH}} - \Delta G^{\circ}.$

^e From O'Callaghan et al. (2001).

^fFrom Willcox et al. (1999). Δ H $^{\circ}$ value determined by isothermal titration calorimetry; $T\Delta$ S $^{\circ} = \Delta$ H $^{\circ}$ - Δ G $^{\circ}$.

⁹ From Boniface et al. (1999). K_D calculated from reported thermodynamic parameters.

^h From Garcia et al. (2001).

From Anikeeva et al. (2003).

Table 2. Heat-Capacity Changes and Entropy Terms for Immunoreceptor-Ligand Complexes

Receptor-Ligand	$-\Delta \textbf{A}_{np}{}^{a}$	$-\Delta \textbf{A}_{\text{p}}{}^{\text{a}}$	$\Delta C^{\circ}_{\ p\ calc}{}^{b}$	$\Delta C^{\circ}_{\ p\ obs}{}^{c}$	T _s ^c	$\Delta \text{S}^{\circ}_{\text{HE}} \ (\text{T}_{\text{s}})^{\text{d}}$	$\Delta \textbf{S}^{\circ}_{~Tr}$	$\Delta { m S}^{\circ}_{ m other}$ (${ m T_s}$) $^{ m e}$	$\Re^{\mathfrak{f}}$
	(Ų)	(Ų)	(cal/mol K)	(cal/mol K)	(K)	(cal/mol K)	(^{cal} / _{mol K})	(cal/mol K)	
huNKG2D-MIC-A	1267	1017	-263	-828 ± 155	306	259	-50	-209	37
huNKG2D-MIC-B	994	960	-184	-344 ± 146	320	87	-50	-37	7
huNKG2D-ULBP1	1095	805	-238	-221 ± 139	323	53	-50	-3	1
muNKG2D-RAE-1β TCR-MHC-Peptide	1045	636	-245	-218 ± 64	319	55	-50	-6	1
2B4-H2-E ^k -MCC ^g	1226	762	-286	-663 ± 53	290	256	-50	-206	37
172.10-H2-A ^u -MBP1 ^h	_	_	_	-159	220	120	-50	-70	13
1934.4-H2-A ^u -MBP1 ^h	_	_	_	-1248	290	479	-50	-429	77
D3-HLA-A2-SL9i	_	_	_	-363	283	152	-50	-102	18

^aChange in water-accessible surface area (np = nonpolar, p = polar) upon binding, calculated from structural data (complex structures available for MIC-A and RAE-1β; MIC-B superimposed on MIC-A complex structure; ULBP1 calculated using ULBP3 complex structure; and H2-E^k-MCC from model of 2B4 on 2C-K^b template superimposed on H2-E^k structure (Boniface et al., 1999).

nant (–5.2 to –5.9 kcal/mol). MIC-A, due to its higher heat capacity, has become completely enthalpy driven at 37°C (–11.5 kcal/mol), and entropy has become a smaller, negative contribution to binding (T Δ S° = 3.1 kcal/mol). Even at physiological temperatures, only MIC-A deviates from an NKG2D binding mode combining contributions from both enthalpy and entropy.

Heat Capacities of NKG2D-Ligand Interactions Reveal Variations in the Amount of Local Folding Upon Binding

The degree of curvature in the three-parameter fits (Figure 1D) correlates with $\Delta C^{\circ}_{P \text{ obs}}$ (Table 2). The overwhelming effect of liberating water clathrates by burial of hydrophobic surfaces at most binding interfaces causes a negative $\Delta C^{\circ}_{P obs}$ that dominates over entropy $(\Delta C^{\circ}_{Pobs}>> \Delta S)$, resulting in entropy/enthalpy compensation and characteristic extrema in plots of ΔG and K_D versus T at points termed T_S and T_H, respectively (Ha et al., 1989). T_S is the temperature at which $\Delta S^{\circ} = 0$, where the binding process is entirely enthalpy driven; conversely, T_H occurs where $\Delta H^{\circ} = 0$. The minimum for the NKG2D-MIC-A interaction in Figure 1D represents the T_s; for the other three NKG2D-ligand interactions, T_s is located above the experimental temperature range (Table 2). Likewise, T_H values are characteristically low for these four NKG2D-ligand interactions, ranging from 283 K for Rae-1β to 296 K for MIC-A (data not shown; compare to Table 2 in Ha et al., 1989).

 $\Delta C^{\circ}_{\mbox{\tiny Pobs}}$ for a particular interaction can be further broken down into contributions from the burial of accessible surface area at the binding interface due to complexation or the burial of hydrophobic surface due to local protein folding events at the interface; the former value can be estimated from the extent of the binding interface

and its polar/nonpolar characteristics (Spolar and Record, 1994). The polar/nonpolar character of the buried surfaces was calculated directly from the complex structures for huNKG2D-MIC-A and muNKG2D-RAE-1 β ; for huNKG2D-MIC-B, it was estimated by docking the unliganded structure of MIC-B onto MIC-A in the NKG2D complex structure; and for huNKG2D-ULBP1 from the huNKG2D-ULBP3 complex structure.

The calculated and observed heat capacities for the interaction between NKG2D and ULBP1 or RAE-1β closely match, indicating that these proteins associate as rigid entities. The large deviation between $\Delta C^{\circ}_{P \; calc}$ and ΔC°_{Pobs} for huNKG2D-MIC-A, as well as the smaller, yet significant, deviation for huNKG2D-MIC-B, suggests that some local folding events likely occur concurrent with binding. The scale of these local folding events can be estimated at T_s (see Experimental Procedures; Spolar and Record, 1994). As expected from the correlation of expected and observed heat capacities, the interactions of NKG2D with ULBP1 and RAE-1 are estimated to result in no significant local folding upon binding. However, the folding of approximately 7 residues (huNKG2D-MIC-B) or 37 residues (huNKG2D-MIC-A) is estimated to occur during binding for other complexes.

These results are consistent with structural features of the ligand proteins. The crystal structures of both MIC-A (Li et al., 1999) and MIC-B (Holmes et al., 2002) reveal regions in the $\alpha 2$ helix (residues 152 through 161) that are either less well ordered (for MIC-B, by high relative B factors and choppy electron density) or completely disordered (for MIC-A) in the absence of bound NKG2D. In the huNKG2D-MIC-A complex structure, this region folds into two turns of α -helix and a short stretch of coil, forming a large part of the interface with NKG2D (Li et al., 2001). This region in the unliganded structure of RAE-1 β is well ordered, the result of extensive repack-

 $^{^{\}mathrm{b}}$ Calculated from the equation $\Delta\mathrm{C}^{\circ}_{\,\mathrm{p\,calc}} = (0.32\ \Delta\mathrm{A}_{\mathrm{np}}) - (0.14\ \Delta\mathrm{A}_{\mathrm{p}})$ (Spolar and Record, 1994). Calculation of $\Delta\mathrm{C}^{\circ}_{\,\mathrm{p\,calc}}$ requires a crystal structure or an acceptable model. The huNKG2D-MIC-B model was constructed from the MIC-B and huNKG2D-MIC-A crystal structures as described by Holmes et al. (2002), due to high sequence homology with MIC-A (84% sequence identity). The crystal structure of huNKG2D-ULBP3 was used to calculate values for ULBP1 (55% sequence identity).

 $^{^{\}circ}$ For NKG2D-ligand interactions, from three-parameter fit to data shown in Figure 1D with Δ S $^{\circ}$ held constant. For TCR-pMHC interactions, T $_{s}$ was either reported directly or was calculated from the entropy and heat capacity.

^d $\Delta S^{\circ}_{HE}(T) = 1.35 \Delta C^{\circ}_{p \text{ obs}} \text{ In (T/386 K) (see eq. [3] [Spolar and Record, 1994]).}$

 $^{^{}e}\Delta S^{\circ}_{\text{other}}$ (T_s) = $-[\Delta S^{\circ}_{\text{HE}}$ (T_s) + $\Delta S^{\circ}_{\text{Tr}}$] (Boniface et al., 1999; Spolar and Record, 1994).

^f Residues that fold upon binding estimated from heat capacity according to Spolar and Record, (1994).

⁹ From Boniface et al. (1999).

^h From Garcia et al. (2001).

From Anikeeva et al. (2003).

ing of the RAE-1 hydrophobic core (Li et al., 2002). The structure of ULBP3 is available only as a complex with NKG2D (Radaev et al., 2001), but the analogous segment is presumed to be well ordered by analogy to RAE-1β.

Any removal of protein surface area upon binding is reflected in the $\Delta \text{C}_{\text{P obs}}{}^{\circ}\text{,}$ whereas ΔH° and ΔS° contain information on the overall energetic stabilization of the complex. Since the NKG2D interactions with MIC-A and MIC-B are even more strongly entropically driven than with the well-ordered ligands RAE-1β and (presumably) ULBP1, and since the kinetic studies of NKG2D-MIC-A found no significant energetic barrier to forming the transition state (see below), we propose that this folding event is concurrent with, but does not hinder, NKG2D binding. Alternatively, the thermodynamic differences could be accounted for by nonlocalized conformational changes, such as an increased "breathing" motion in certain bound ligands or changes in the overall flexibility of some complexes that have not been directly observed. However, given the overall structural similarity of NKG2D-ligand interactions, the MIC-A loop is the only directly observed structural difference likely large enough to account for the unusual thermodynamic characteristics of NKG2D-MIC-A complexation.

However, ordering of these loops in MIC-A and -B concurrent with NKG2D binding cannot contribute to an induced-fit mechanism in that (1) the transition appears to be from a disordered state to a *single* ordered state, not multiple conformations induced as complementary to a variety of different ligand/receptor surfaces; and (2) flexibility in one or two *ligand* proteins cannot contribute to recognition degeneracy by a single *receptor*.

Kinetics of the NKG2D-MIC-A Interaction Are Fast and Temperature Insensitive

The dissociation kinetics of three of the four complexes (e.g., for MIC-B in Figure 1A) are too fast to measure reliably with a Biacore 3000 instrument. However, NKG2D-MIC-A interaction kinetics are slow enough to be measured accurately: $k_{on} = 4.3 \times 10^4 \, M^{-1} \, s^{-1}$, $k_{off} =$ 0.023 s⁻¹ (Figures 2A and 2B). The kinetic values obtained at 25°C in this study agree with previous results (Li et al., 2001) and imply a K_D (0.54 μ M) comparable to that determined through equilibrium affinity analysis (0.94 µM from Table 1). The temperature dependence of association and dissociation kinetics, useful for calculating the activation energy barriers for the interaction, were measured over a temperature range of 283 to 310 K (Figures 2C and 2D). The slopes of these plots are equal to the activation energy divided by the gas constant (R), giving activation energies of 5.7 kcal/mol for association and 9.6 kcal/mol for dissociation (Figure 2E).

Discussion

NKG2D-Ligand and TCR-pMHC Binding Display Fundamentally Different Thermodynamics and Kinetics

Using SPR, we found the affinities of huNKG2D for three huNKG2D ligands (MIC-A, MIC-B, and ULBP1) and of muNKG2D for one muNKG2D ligand (RAE-1 β) to be in the high nanomolar to very low micromolar range (Table 1), consistent with previously reported values (Carayan-

nopoulos et al., 2002b; O'Callaghan et al., 2001; Radaev et al., 2002; Strong, 2002), and generally stronger than the mid-to-low micromolar K_Ds reported for TCR-pMHC binding (Rudolph et al., 2002) (Table 1). Buried surface area at TCR-pMHC interfaces is generally slightly less than that at NKG2D-ligand interfaces, although the two ranges overlap (1600 to 1900 Å² for 11 TCR-pMHC, with one 1200 Å² exception [Rudolph et al., 2002]; 1700 to 2200 Å² for NKG2D-ligand [McFarland et al., 2003]). The NKG2D-ligand interfaces are also not strikingly hydrophobic in character, even less so than previously studied TCR-pMHC interfaces, reflecting similar $\Delta C^{\circ}_{P calc}$ values (Table 2). An average of 58% of the surface area buried at NKG2D-ligand interfaces is nonpolar, closely matching the average nonpolar character (54%) of the total ligand solvent-accessible surfaces and comparable to the 62% nonpolar buried surface area at the 2B4-H2-E^k-MCC interface (Boniface et al., 1999). The three NKG2D-ligand complexes are also more shape complementary (Sc = 0.63 to 0.72) than nine TCR-pMHC class I complexes (Sc = 0.41 to 0.66) and two of three TCR-pMHC class II complexes (Sc = 0.56 to 0.71) (Rudolph et al., 2002).

For TCR-pMHC, analyzing the variation of affinity with temperature, by both conventional (Willcox et al., 1999) and multiparameter (Anikeeva et al., 2003; Boniface et al., 1999; Garcia et al., 2001) van't Hoff methods, revealed a large enthalpic driving force tempered by an unfavorable entropic term, characteristic of induced-fit binding (Table 1). In contrast, both methods rather show that entropy is the primary driving force for all four NKG2D-ligand interactions tested, and that the magnitude of the favorable enthalpic term is markedly smaller. The change of sign for the entropic term implies that modes of configurational freedom are being gained by the system upon binding, where, with TCR-pMHC, configurational freedom was lost. The dramatic opposition of enthalpy and entropy in TCR-pMHC interactions was used as evidence that a flexible interface was stabilized, or "frozen," upon complex formation (Anikeeva et al., 2003; Boniface et al., 1999; Willcox et al., 1999), much like induced-fit antibody-antigen interactions. In contrast, all the NKG2D-ligand interactions analyzed here fall within the range of the thermodynamic characteristics of 30 nonantibody, rigid protein-rigid protein interactions (Figure 3). The three thermodynamic parameters derived from the multi-parameter fit (ΔH° , ΔS° , and ΔC_{P}°) can be summarized as T_s values (see Results). The two reported T_S values for TCR-pMHC interactions are 283 K and 290 K (Anikeeva et al., 2003; Boniface et al., 1999). T_s values for NKG2D-ligand complexes are about 20 to 40 degrees higher, with the exception of \sim 5 degrees for MIC-A, again inconsistent with induced-fit interactions.

TCR-pMHC association kinetics ($k_{on} \sim 10^2$ to 10^4 M $^{-1}$ s $^{-1}$, $k_{off} \sim 0.1$ to 0.01 s $^{-1}$) (Davis et al., 1998; Willcox et al., 1999) are generally slower than those for NKG2D-ligands. The sluggish nature of TCR-pMHC kinetics is consistent with induced-fit recognition (Boniface et al., 1999; Willcox et al., 1999); in contrast, the velocity of NKG2D-ligand complex formation ($k_{on} > 10^5$ M $^{-1}$ s $^{-1}$ for MIC-B, ULBP1, and Rae-1 β ; see Figure 1A) was an early indicator that induced-fit binding was not occurring. An induced-fit interaction is expected to have a high activation energy due to the energetic cost of ordering a flexi-

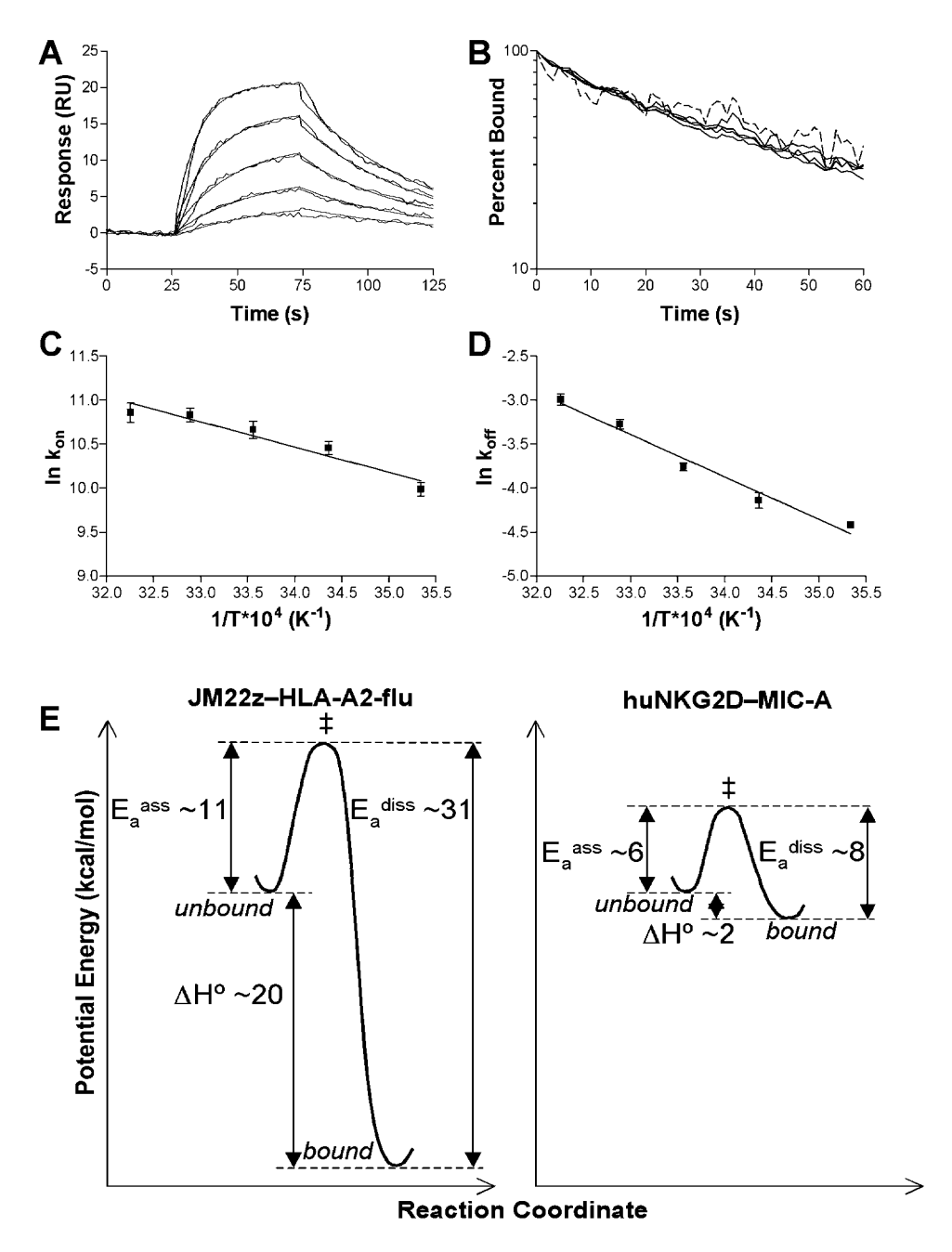


Figure 2. Temperature Dependence of NKG2D-MIC-A Kinetics

(A) huNKG2D was injected at 80 μ l/min over a MIC-A-coupled dextran surface in five serial dilutions ranging from 2.5 μ M to 0.16 μ M. The response of an in-line HLA-G control surface was subtracted. Data are shown for 298 K.

(B) huNKG2D dissociation response (data from Figure 2A, time normalized to the beginning of dissociation phase) exhibits monophasic exponential kinetics. The dashed line is the dissociation for the lowest concentration (0.16 μM), where instrument noise is significant. (C and D) Arrhenius plots of association and dissociation rates over a range of temperatures from 283 to 310 K.

(E) Reaction profiles, to scale, of potential energy for the JM22z-HLA-A2-flu TCR-pMHC interaction from (Willcox et al., 1999) (left) and the NKG2D-MIC-A interaction (right). E_a^{ass} , energy of association; E_a^{diss} , energy of dissociation; double dagger, high-energy intermediate.

ble molecule into a smaller manifold of transition-state conformations, and the Arrhenius activation energy calculated for JM22z TCR association with pMHC is high at 11 kcal/mol (Willcox et al., 1999). However, the energy of association for the NKG2D-MIC-A interaction is 5.7 kcal/mol, closer to the diffusion limit of $\sim\!\!5$ kcal/mol (Longsworth, 1954), indicating that the NKG2D-ligand transition state is more accessible (Figure 2E).

Therefore, of the four thermodynamic or kinetic characteristics recognized as indicators of an induced-fit binding mechanism for TCR-pMHC interactions $(\Delta H^\circ, \Delta S^\circ, \, \Delta C_{P}^\circ,$ and activation energy), only one value for one of the four NKG2D-ligand complexes tested here exhibited similar values $(\Delta C_{P}^\circ$ for NKG2D-MIC-A)—which can be explained by structural aspects of the ligand protein, not the receptor. We therefore conclude

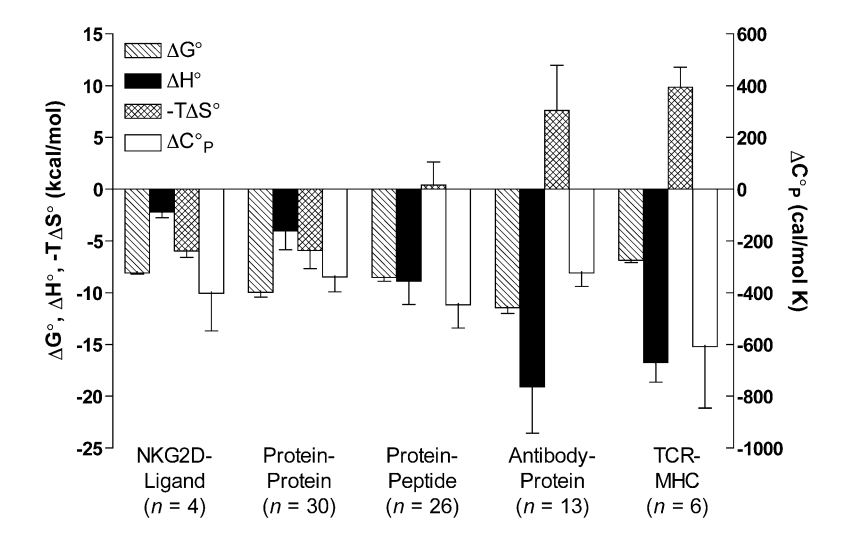


Figure 3. Comparison of Thermodynamic Parameters for Several Classes of Binding Interactions

Average values for ΔG° , ΔH° , $-T\Delta S^{\circ}$, and ΔC°_{P} are given for five classes of protein-ligand interactions calculated from the number of data points n (ΔC°_{P} values were calculated for n = 4, 16, 13, 13, and 4, from left to right). Spontaneous binding energy increases in a negative direction. Error bars represent SEM. Data for NKG2D-ligand interactions are average values from Tables 1 and 2. Data for peptide-protein interactions, antibody-antigen interactions, and other protein-protein interactions are from a table compiled by Stites (1997). Data for TCR-pMHC interactions obtained from Anikeeva et al. (2003), Boniface et al. (1999), Garcia et al. (2001), and Willcox et al. (1999). All values for 298 K except for compiled values, which were obtained in the range 287.3 to 303 K.

that none of the NKG2D-ligand complexes exhibit the thermodynamic signatures associated with induced-fit interactions.

Rigid Adaptation of NKG2D to Multiple Ligands Explains Degeneracy

In the absence of the dominance of hydrophobic or electrostatic interface interactions, and without utilizing induced-fit binding, NKG2D recognition degeneracy is likely best explained by an extension of the mechanism described for the interactions between antibody Fc domains and various proteins (DeLano et al., 2000). This study showed that a single protein binding site is capable of degenerately interacting with at least four distinct protein ligands, in the absence of any major flexibility, partly by using aromatic residues, capable of making several different types of interactions, on both halves of the interface to form contacts across hydrophobic binding sites. However, NKG2D-ligand interactions are extreme examples of this type of binding mechanism, where the interfaces are more extensive and complementary, and also include significant proportions of salt bridges and geometry-specific hydrogen bonds.

At the center of the NKG2D binding site lie two conserved tyrosine residues (152 and 199 in huNKG2D) that constitute the dominant binding energy "hotspots" (Clackson and Wells, 1995) in each complex half-site (McFarland et al., 2003). These two tyrosines are held fairly rigid in the NKG2D structure, where the only significant conformational change observed is utilization of a single alternate rotamer by Tvr152 in two of the total of eight crystallographic views of NKG2D (McFarland et al., 2003). As has been seen in many antibody combining sites (Nikula et al., 1995; Padlan, 1990), these tyrosines are capable of making multifarious interactions with distinct ligand surfaces (Figure 4). In all six complex halfsites, this pair of tyrosines sandwich a ligand residue, but this residue varies from hydrophobic methionines (in two different rotamers) or a leucine, to an alanine, to a phenylalanine (making both en face and herringbone ring-stacking interactions), to even an arginine (making cation-π interactions (Gallivan and Dougherty, 1999) with both tyrosines). In addition to these sandwich interactions, the side-chains of these two tyrosines participate in additional hydrogen bonds and hydrophobic contacts, distinct across the six complex half-sites.

NKG2D recognition degeneracy is therefore achieved by investing a significant proportion of the binding energy in core residues that, while rigidly constrained, are capable of making specific, yet disparate, interactions with divergent ligand binding surfaces. These core interactions are placed within the context of extensive, highly shape-complementary interfaces, where additional electrostatic, hydrogen, and van der Waals bonds contribute to the overall affinity while minimizing the dominance of any single peripheral bond. The extent of the interfaces contribute to affinity and specificity by enabling multiple peripheral bonds to add to affinity, but also by requiring that potential target ligands stringently exclude deleterious steric clashes, both on the scale of individual side-chains and in the overall shape of the NKG2D binding saddle (McFarland et al., 2003). Thus, NKG2D has evolved to utilize a recognition mechanism that is capable of specifically binding to diverse ligands while tolerating considerable ligand interface sequence variation. The latter phenomena may allow the immune system to fine tune the NKG2D activation threshold through subtle alteration of the kinetics and affinities of particular interactions in specific contexts.

This extreme degenerate recognition is achieved within an essentially rigid receptor binding site structure. Therefore, we term this mode of binding rigid adaptation. NKG2D is a dominantly activating immunoreceptor, where NKG2D engagement delivers strongly activating signals to effector cells. Utilizing rigid adaptation recognition in this context has the distinct advantage that, while allowing for degeneracy to expand the repertoire of potential NKG2D ligands, thus extending the utility of NKG2D signaling, and allowing for subtle modulation of NKG2D signals through peripheral sequence variation, this recognition machinery precludes the crossreactivity inherent in induced-fit binding (Boniface et al., 1999; James et al., 2003; Wu et al., 2002), preventing the inappropriate NKG2D-mediated elimination of nonbona fide cellular targets. Thus, the immune system has developed an elegant system delivering broad utility

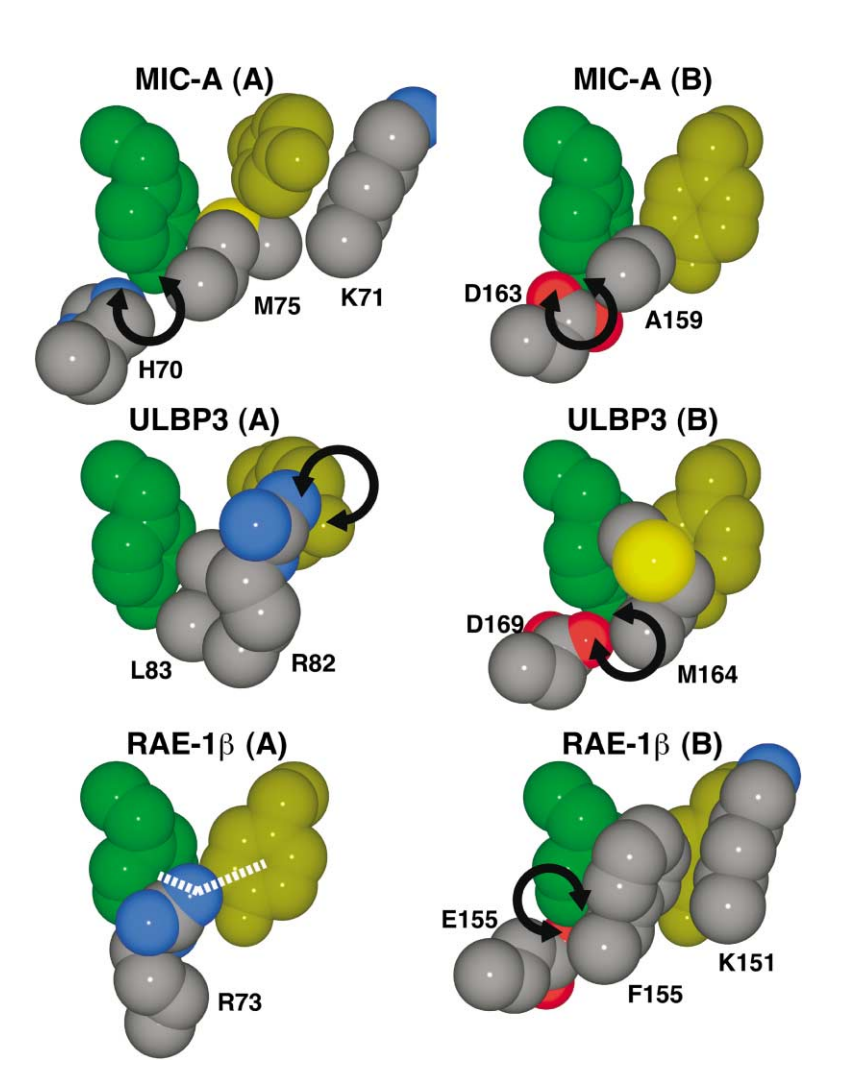


Figure 4. Interactions of Core Tyrosine Residues with Different Ligand Surfaces

Space-filling views of selected residues from the core area of NKG2D-ligand interfaces. Coordinates derived from the following crystal structures: NKG2D-MIC-A (PDB accession number 1HYR), NKG2D-ULBP3 (1KCG), and NKG2D-RAE-1 β (1JSK). Each crystal structure depicts two NKG2D sites interacting with ligand; (A) is the site located over the $\alpha 1$ domain and (B) is the site located over the $\alpha 2$ domain. Homologous core tyrosines from NKG2D are colored green (human 199, mouse 215) or dark yellow (human 152, mouse 168); ligand are atoms colored by atom type (carbon, gray; nitrogen, blue; oxygen, red; sulfur, yellow). For MIC-A(A) and ULBP3(A), Tyr152 is probably rotated from its ground state by contact with ligand at energetic cost (McFarland et al., 2003). The following residues depicted are within normal hydrogen bonding distance (shown by arrows): for MIC-A(A), Y199 and H70: for MIC-A(B), Y199 and D163; for ULBP3(A), Y152 and R82; for ULBP3(B), Y199 and D169; for RAE-1β(B), Y215 and E155. Cation- π interactions in the RAE-1_B(A) half-site are shown as dashed white lines. Additional hydrophobic interactions are formed between Y152 and K71 in MIC-A(A) and between Y168 and K151 in RAE-1β(B).

while minimizing potentially deleterious responses, mirroring the functionally distinct recognition mechanisms utilized by TCRs or antibodies.

Experimental Procedures

Protein Expression and Purification

Soluble forms of the extracellular domains (huNKG2D, residues 80 through 216; muNKG2D, residues 99 through 234; MIC-A, allele 001, residues 1 through 276; MIC-B, allele 005, residues 1 through 274; ULBP1, residues 1 through 180; and RAE-1 β , residues 1 through 178), truncated proximal to transmembrane spanning segments and including exogenous N-terminal initiator methionines, were refolded in vitro from bacterial inclusion bodies and purified as described (Holmes et al., 2002; Li et al., 2001, 2002; Steinle et al., 2001), Ligand protein constructs also included C-terminal six-residue polyhistidine purification tags. To ensure the monodispersivity of proteins used for SPR, all protein samples were purified by size-exclusion chromatography in HBS-EA buffer (10 mM HEPES [pH 7.4], 150 mM NaCl, 3 mM EDTA, and 0.02% NaN₃) within 48 hr of use. Protein concentration was determined by BCA protein assay (Pierce; Rockford, IL) and 0.05% P-20 surfactant (BIAcore AB; Uppsala, Sweden) was added to each protein sample.

SPR Measurements

SPR measurements were carried out in HBS-EP buffer (10 mM HEPES [pH 7.4], 150 mM NaCl, 3 mM EDTA, and 0.05% P-20; Biacore AB; Uppsala, Sweden) using a Biacore 3000 system (Biacore AB). All NKG2D ligands and binding controls were coupled to research-

grade CM5 sensor chips using amine coupling chemistry. A soluble form of HLA-G was coupled in a flow cell adjacent to each NKG2D ligand as a negative binding control. Human or muNKG2D was injected under standard buffer conditions identical to previous studies (Boniface et al., 1999; Willcox et al., 1999).

Affinity analyses were carried out using ligand coupling densities resulting in maximum analyte response values (R_{max}) of $\sim\!25$ response units (RU) for MIC-A to $\sim\!500$ RU for MIC-B. Responses reached equilibrium within 30 to 40 μ l injections of analyte (NKG2D, at 15 μ A/min). The average equilibrium responses were measured for five to six NKG2D concentrations bracketing the K_D of each ligand. A plot of response versus [NKG2D] was fit to a simple steady state binding model using BIAevaluation 3.0 software (Biacore AB). The K_D was determined in three to four independent experiments for each of nine temperatures ranging from 283 to 310 K.

The kinetics of the NKG2D-MIC-A interaction were measured using a low MIC-A density to minimize mass transport effects. The lack of concentration dependence shown in Figure 2B argues against a mass transport effect, as does an experiment where huNKG2D was injected over the MIC-A surface at flow rates from 5 to 75 μ λ/min, resulting in no change in association or dissociation kinetics (data not shown). Also, the complex dissociation rate was constant regardless of NKG2D injection time (between 1 and 20 min; data not shown). Four to five NKG2D concentrations (40 μ l injections at 80 μ l/min) were used for each determination of on- and off-rates by global fitting using the 1:1 Langmuir binding model in BIAevaluation 3.0, and rate constants were determined three times independently at each of five temperatures ranging from 283 to 310 K. Arrhenius plots were fit using the linear regression algorithm in Prism 3 (GraphPad Software; San Diego, CA).

Thermodynamic Calculations

 K_{D} values were converted to ΔG values as $\Delta G = \text{-RT In } K_{\text{D}}$ and plotted versus T for the three-parameter fit, as in Boniface et al. (1999), Spolar and Record (1994), and Yoo and Lewis (1995). Nonlinear regression in Prism 3 (GraphPad Software) was used to fit the following equation to the data:

$$\Delta \text{G}^{\circ}_{\text{ T}} = \Delta \text{H}^{\circ}_{\text{ T}_{\text{R}}} + \Delta \text{C}^{\circ}_{\text{ P}} \left(\text{T} - \text{T}_{\text{R}}\right) - \text{T}\Delta \text{S}^{\circ}_{\text{ T}_{\text{R}}} - \text{T}\Delta \text{C}^{\circ}_{\text{ P}} \text{ In (T/T}_{\text{R}}) \quad \text{(4)}$$

where T_R is a constant reference temperature, and the three fit parameters are ΔH°_{TR} , the change in enthalpy upon binding at T_R ; ΔS°_{TR} , the change in entropy upon binding at T_R ; and ΔC°_{P} , the change in heat capacity. Starting values for the three parameters did not affect the final values. In equation 6 we have not explicitly included a $\Delta C^{\circ}_{P}/dT$ term, making the assumption that ΔC°_{P} does not change with temperature, since including this term during fitting results in (1) $\Delta C^{\circ}_{P}/dT$ values that are zero within the error of the estimate and (2) higher standard errors overall for the three other parameters. Similar behavior has been observed for TCR-pMHC (Boniface et al., 1999) and protein-peptide (Yoo and Lewis, 1995) interactions.

The number of residues folding upon binding is estimated using the following equation:

$$\Delta \mathbf{S}^{\circ} = \Delta \mathbf{S}^{\circ}_{\text{HE}} + \Delta \mathbf{S}^{\circ}_{\text{Tr}} + \Delta \mathbf{S}^{\circ}_{\text{other}} \tag{5}$$

where $\Delta S^{\circ}_{\text{HE}}$ is the change in entropy due to hydrophobic burial, determined from $\Delta C^{\circ}_{\text{Pobs}}$ and T_{S} at a given temperature (Spolar and Record, 1994) (Table 2) and $\Delta S^{\circ}_{\text{Tr}}$ is the change in entropy from loss of translational and rotational degrees of freedom upon binding, constant for a 1:1 binding interaction at –50 $^{\text{cal}} I_{\text{mol K}}$ (Boniface et al., 1999; Spolar and Record, 1994). Remaining entropic effects, such as changes in conformational entropy, are accounted for by the $\Delta S^{\circ}_{\text{other}}$ term. It is particularly convenient to calculate these values at T_{S} where $\Delta S^{\circ}=0$ (Boniface et al., 1999):

$$\Delta S^{\circ}_{HE} + \Delta S^{\circ}_{Tr} = \Delta S^{\circ}_{other}.$$
 (6)

In protein-DNA and protein-protein interactions, folding of amino acid residues upon binding is the major component of $\Delta S^{\circ}_{\text{other}}$ so that the number of residues that fold upon binding ()}) can be calculated from $\Delta S^{\circ}_{\text{other}}$ using an estimate of –5.6 $^{\text{cal}}/_{\text{mol K}}$ for entropic loss from the folding of a single residue (Spolar and Record, 1994).

Acknowledgments

This work was supported by NIH grant Al48675 (R.K.S.) and a post-doctoral fellowship from the Cancer Research Institute (B.J.M.).

Received: July 15, 2003 Revised: September 17, 2003 Accepted: October 16, 2003 Published: December 9, 2003

References

Alexander, J.M., Nelson, C.A., van Berkel, V., Lau, E.K., Studts, J.M., Brett, T.J., Speck, S.H., Handel, T.M., Virgin, H.W., and Fremont, D.H. (2002). Structural basis of chemokine sequestration by a herpesvirus decoy receptor. Cell 111, 343–356.

Anikeeva, N., Lebedeva, T., Krogsgaard, M., Tetin, S.Y., Martinez-Hackert, E., Kalams, S.A., Davis, M.M., and Sykulev, Y. (2003). Distinct molecular mechanisms account for the specificity of two different T-cell receptors. Biochemistry *42*, 4709–4716.

Bauer, S., Groh, V., Wu, J., Steinle, A., Phillips, J.H., Lanier, L.L., and Spies, T. (1999). Activation of NK cells and T cells by NKG2D, a receptor for stress-inducible MICA. Science 285, 727–729.

Boniface, J.J., Reich, Z., Lyons, D.S., and Davis, M.M. (1999). Thermodynamics of T cell receptor binding to peptide-MHC: evidence for a general mechanism of molecular scanning. Proc. Natl. Acad. Sci. USA 96. 11446–11451.

Carayannopoulos, L.N., Naidenko, O.V., Fremont, D.H., and Yoko-yama, W.M. (2002a). Cutting edge: murine UL16-binding protein-

like transcript 1: a newly described transcript encoding a high-affinity ligand for murine NKG2D, J. Immunol, 169, 4079–4083.

Carayannopoulos, L.N., Naidenko, O.V., Kinder, J., Ho, E.L., Fremont, D.H., and Yokoyama, W.M. (2002b). Ligands for murine NKG2D display heterogeneous binding behavior. Eur. J. Immunol. 32, 597–605.

Cerwenka, A., and Lanier, L.L. (2001). Natural killer cells, viruses and cancer. Nat. Rev. Immunol. 1, 41–49.

Clackson, T., and Wells, J.A. (1995). A hot spot of binding energy in a hormone-receptor interface. Science 267, 383–386.

Cosman, D., Mullberg, J., Sutherland, C.L., Chin, W., Armitage, R., Fanslow, W., Kubin, M., and Chalupny, N.J. (2001). ULBPs, novel MHC class I-related molecules, bind to CMV glycoprotein UL16 and stimulate NK cytotoxicity through the NKG2D receptor. Immunity 14, 123–133.

Das, H., Groh, V., Kuijl, C., Sugita, M., Morita, C.T., Spies, T., and Bukowski, J.F. (2001). MICA engagement by human $V\gamma 2V\delta 2$ T cells enhances their antigen-dependent effector function. Immunity *15*, 83–93.

Davis, M.M., Boniface, J.J., Reich, Z., Lyons, D., Hampl, J., Arden, B., and Chien, Y. (1998). Ligand recognition by $\alpha\beta$ T cell receptors. Annu. Rev. Immunol. *16*, 523–544.

DeLano, W.L., Ultsch, M.H., de Vos, A.M., and Wells, J.A. (2000). Convergent solutions to binding at a protein-protein interface. Science 287, 1279–1283.

Diefenbach, A., Jamieson, A.M., Liu, S.D., Shastri, N., and Raulet, D.H. (2000). Ligands for the murine NKG2D receptor: expression by tumor cells and activation of NK cells and macrophages. Nat. Immunol. 1, 119–126.

Gallivan, J.P., and Dougherty, D.A. (1999). Cation-pi interactions in structural biology. Proc. Natl. Acad. Sci. USA 96, 9459–9464.

Garcia, K.C., Degano, M., Pease, L.R., Huang, M., Peterson, P.A., Teyton, L., and Wilson, I.A. (1998). Structural basis of plasticity in T cell receptor recognition of a self peptide-MHC antigen. Science 279, 1166–1172.

Garcia, K.C., Radu, C.G., Ho, J., Ober, R.J., and Ward, E.S. (2001). Kinetics and thermodynamics of T cell receptor- autoantigen interactions in murine experimental autoimmune encephalomyelitis. Proc. Natl. Acad. Sci. USA 98, 6818–6823.

Groh, V., Rhinehart, R., Randolph-Habecker, J., Topp, M.S., Riddell, S.R., and Spies, T. (2001). Costimulation of CD8 $\alpha\beta$ T cells by NKG2D via engagement by MIC induced on virus-infected cells. Nat. Immunol. 2, 255–260.

Groh, V., Wu, J., Yee, C., and Spies, T. (2002). Tumour-derived soluble MIC ligands impair expression of NKG2D and T-cell activation. Nature 419, 734–738.

Ha, J.H., Spolar, R.S., and Record, M.T., Jr. (1989). Role of the hydrophobic effect in stability of site-specific protein-DNA complexes. J. Mol. Biol. 209, 801–816.

Hayakawa, Y., Kelly, J.M., Westwood, J.A., Darcy, P.K., Diefenbach, A., Raulet, D., and Smyth, M.J. (2002). Cutting edge: tumor rejection mediated by NKG2D receptor-ligand interaction is dependent upon perforin. J. Immunol. *169*, 5377–5381.

Henriques, D.A., Ladbury, J.E., and Jackson, R.M. (2000). Comparison of binding energies of SrcSH2-phosphotyrosyl peptides with structure-based prediction using surface area based empirical parameterization. Protein Sci. 9, 1975–1985.

Holmes, M.A., Li, P., Petersdorf, E.W., and Strong, R.K. (2002). Structural studies of allelic diversity of the MHC class I homolog MIC-B, a stress-inducible ligand for the activating immunoreceptor NKG2D. J. Immunol. *169*. 1395–1400.

James, L.C., Roversi, P., and Tawfik, D.S. (2003). Antibody multispecificity mediated by conformational diversity. Science 299, 1362– 1367.

Jan Chalupny, N., Sutherland, C.L., Lawrence, W.A., Rein-Weston, A., and Cosman, D. (2003). ULBP4 is a novel ligand for human NKG2D. Biochem. Biophys. Res. Commun. 305, 129–135.

Kasahara, M., Watanabe, Y., Sumasu, M., and Nagata, T. (2002). A family of MHC class I-like genes located in the vicinity of the mouse

leukocyte receptor complex. Proc. Natl. Acad. Sci. USA 99, 13687–13692.

Li, P., Willie, S.T., Bauer, S., Morris, D.L., Spies, T., and Strong, R.K. (1999). Crystal structure of the MHC class I homolog MIC-A, a $\gamma\delta$ T cell ligand. Immunity *10*, 577–584.

Li, P., Morris, D.L., Willcox, B.E., Steinle, A., Spies, T., and Strong, R.K. (2001). Complex structure of the activating immunoreceptor NKG2D and its MHC class I-like ligand MICA. Nat. Immunol. 2, 443–451.

Li, P., McDermott, G., and Strong, R.K. (2002). Crystal structures of RAE-1 β and its complex with the activating immunoreceptor NKG2D. Immunity 16, 77–86.

Longsworth, L.G. (1954). Temperature dependence of diffusion in aqueous solutions. J. Phys. Chem. 58, 770–773.

McFarland, B.J., Kortemme, T., Yu, S.F., Baker, D., and Strong, R.K. (2003). Symmetry recognizing asymmetry. Analysis of the interactions between the C-type Lectin-like immunoreceptor NKG2D and MHC class I-like ligands. Structure *11*, 411–422.

Nikula, T.K., Bocchia, M., Curcio, M.J., Sgouros, G., Ma, Y., Finn, R.D., and Scheinberg, D.A. (1995). Impact of the high tyrosine fraction in complementarity determining regions: measured and predicted effects of radioiodination on IgG immunoreactivity. Mol. Immunol. 32. 865–872.

O'Callaghan, C.A., Cerwenka, A., Willcox, B.E., Lanier, L.L., and Bjorkman, P.J. (2001). Molecular competition for NKG2D: H60 and RAE1 compete unequally for NKG2D with dominance of H60. Immunity 15, 201–211.

Padlan, E.A. (1990). On the nature of antibody combining sites: unusual structural features that may confer on these sites an enhanced capacity for binding ligands. Proteins 7, 112–124.

Radaev, S., Rostro, B., Brooks, A.G., Colonna, M., and Sun, P.D. (2001). Conformational plasticity revealed by the cocrystal structure of NKG2D and its class I MHC-like ligand ULBP3. Immunity *15*, 1039–1049.

Radaev, S., Kattah, M., Zou, Z., Colonna, M., and Sun, P.D. (2002). Making sense of the diverse ligand recognition by NKG2D. J. Immunol. *169*, 6279–6285.

Reiser, J.B., Gregoire, C., Darnault, C., Mosser, T., Guimezanes, A., Schmitt-Verhulst, A.M., Fontecilla-Camps, J.C., Mazza, G., Malissen, B., and Housset, D. (2002). A T cell receptor CDR3 β loop undergoes conformational changes of unprecedented magnitude upon binding to a peptide/MHC class I complex. Immunity 16, 345–354.

Rini, J.M., Schulze-Gahmen, U., and Wilson, I.A. (1992). Structural evidence for induced fit as a mechanism for antibody-antigen recognition. Science *255*, 959–965.

Rudolph, M.G., Luz, J.G., and Wilson, I.A. (2002). Structural and thermodynamic correlates of T cell signaling. Annu. Rev. Biophys. Biomol. Struct. *31*, 121–149.

Salih, H.R., Rammensee, H.G., and Steinle, A. (2002). Cutting edge: down-regulation of MICA on human tumors by proteolytic shedding. J. Immunol. *169*, 4098–4102.

Skelton, N.J., Quan, C., Reilly, D., and Lowman, H. (1999). Structure of a CXC chemokine-receptor fragment in complex with interleukin-8. Struct. Fold. Des. 7, 157–168.

Somers, W., Ultsch, M., De Vos, A.M., and Kossiakoff, A.A. (1994). The X-ray structure of a growth hormone-prolactin receptor complex. Nature *372*, 478–481.

Spolar, R.S., and Record, M.T., Jr. (1994). Coupling of local folding to site-specific binding of proteins to DNA. Science 263, 777–784.

Steinle, A., Li, P., Morris, D.L., Groh, V., Lanier, L.L., Strong, R.K., and Spies, T. (2001). Interactions of human NKG2D with its ligands MICA, MICB, and homologs of the mouse RAE-1 protein family. Immunogenetics 53, 279–287.

Stites, W.E. (1997). Protein-protein interactions: interface structure, binding thermodynamics, and mutational analysis. Chem. Rev. 97, 1233–1250

Strong, R.K. (2002). Asymmetric ligand recognition by the activating natural killer cell receptor NKG2D, a symmetric homodimer. Mol. Immunol. *38*, 1029–1037.

Sundberg, E.J., and Mariuzza, R.A. (2000). Luxury accommodations: the expanding role of structural plasticity in protein-protein interactions. Struct. Fold. Des. 8, R137–R142.

Sundberg, E.J., and Mariuzza, R.A. (2002). Molecular recognition in antibody-antigen complexes. Adv. Protein Chem. *61*, 119–160.

Willcox, B.E., Gao, G.F., Wyer, J.R., Ladbury, J.E., Bell, J.I., Jakobsen, B.K., and van der Merwe, P.A. (1999). TCR binding to peptide-MHC stabilizes a flexible recognition interface. Immunity 10, 357–365

Wolan, D.W., Teyton, L., Rudolph, M.G., Villmow, B., Bauer, S., Busch, D.H., and Wilson, I.A. (2001). Crystal structure of the murine NK cell-activating receptor NKG2D at 1.95 A. Nat. Immunol. 2, 248–254.

Wu, L.C., Tuot, D.S., Lyons, D.S., Garcia, K.C., and Davis, M.M. (2002). Two-step binding mechanism for T-cell receptor recognition of peptide MHC. Nature *418*, 552–556.

Yoo, S.H., and Lewis, M.S. (1995). Thermodynamic study of the pH-dependent interaction of chromogranin A with an intraluminal loop peptide of the inositol 1,4,5-trisphosphate receptor. Biochemistry 34, 632–638.